Geomechanics and Engineering, *Vol. 12, No. 4 (2017) 595-609*
DOI: https://doi.org/10.12989/gae.2017.12.4.595

Field monitoring of splitting failure for surrounding rock masses and applications of energy dissipation model

Zhi-shen Wang [1a], Yong Li [*1,2], Wei-shen Zhu [1b], Yi-guo Xue [1c], Bei Jiang [1d] and Yan-bo Sun [3e]

[1] *Geotechnical & Structural Engineering Research Center, Shandong University, No. 17923 Jingshi Rd., Jinan, Shandong Province, P.R. China*
[2] *School of Civil Engineering, Shandong University, No. 17922 Jingshi Rd., Jinan, Shandong Province, P.R. China*
[3] *Shandong Luqiao Group CO. LTD, No. 330 Jingwu Road Jinan, P.R. China*

(*Received October 10, 2015, Revised November 16, 2016, Accepted December 02, 2016*)

Abstract. Due to high in-situ stress and brittleness of rock mass, the surrounding rock masses of underground caverns are prone to appear splitting failure. In this paper, a kind of loading-unloading variable elastic modulus model has been initially proposed and developed based on energy dissipation principle, and the stress state of elements has been determined by a splitting failure criterion. Then the underground caverns of Dagangshan hydropower station is analyzed using the above model. For comparing with the monitoring results, the entire process of rock splitting failure has been achieved through monitoring the splitting failure on side walls of large-scale caverns in Dagangshan via borehole TV, micro-meter and deformation resistivity instrument. It shows that the maximum depth of splitting area in the downstream sidewall of the main power house is approximately 14 m, which is close to the numerical results, about 12.5 m based on the energy dissipation model. As monitoring result, the calculation indicates that the key point displacement of caverns decreases firstly with the distance from main powerhouse downstream side wall rising, and then increases, because this area gets close to the side wall of main transformer house and another smaller splitting zone formed here. Therefore it is concluded that the energy dissipation model can preferably present deformation and fracture zones in engineering, and be very useful for similar projects.

Keywords: high geostress; underground cavern group; splitting failure; in-situ monitoring; energy dissipation; opening displacement

1. Introduction

In recent years, the rock mass splitting failure has been often found in the side wall of the underground cavern group of hydropower station in China, such as Yuzixi Hydropower Station,

∗Corresponding author, Associate Professor, Ph.D., E-mail: yongli@sdu.edu.cn
[a] Ph.D. Candidate, B.S.D., E-mail: ashenlittle@126.com
[b] Professor, Ph.D., E-mail: zhuw@sdu.edu.cn
[c] Professor, Ph.D., E-mail: xieagle@sdu.edu.cn
[d] Assistant Professor, Ph.D., E-mail: jiangbei519@qq.com
[e] Senior Engineer, B.S.D., E-mail: 457002533@qq.com

http://www.techno-press.org/?journal=gae&subpage=7 ISSN: 2005-307X (Print), 2092-6219 (Online)

Shisanling Pumped Storage Station and Ertan Hydropower Station (Zhou *et al*. 2008, Li *et al*. 2014, 2015a, b, Wang *et al*. 2016a). Furthermore, the large cracks or nearly perpendicular fracture zone have appeared in the surrounding rock masses in Laxiwa Hydropower Station, Pubugou Hydropower Station and Jinping I Hydroelectric Power Station (Zhou *et al*. 2012, Li *et al*. 2015c, d, 2016a, b, Wang *et al*. 2016b). It is even found that the surrounding rock masses and shotcrete breakdown is widespread in caverns of Jinping II Hydropower Station. These phenomena seriously affected the stability of the underground engineering which is found by Ma *et al*. (2015). In Japan, after analyzing monitoring data of 16 large underground powerhouses, Hibino and Motojma (1995) discovered that it is about 2/3 displacement for igneous and 1/4 displacement for sedimentary rocks in total value of sidewall displacement caused by crack opening, sometimes, which can be reached even 70-80% (Li *et al*. 2011).

It was concluded by Hibino (Hibino and Motojma 1995), a Japanese scholar from the Central Power Institute, who conducted a statistical analysis from institute data of numerous monitoring works for power caverns by borehole TV and extensometer. The research results show that there exists opening deformation inside the rock wall of cavern.

Zhu *et al*. (2011a) found that there may appear the other three engineering hazards caused by cracks and relaxation area beside direct harmness to rock stability. Firstly, the foundation of crane beam might be located on the relaxation rupture zone, which makes the crane beam instable and lacking capacity such as in Pubugou Hydropower Station and Jinping I Hydropower Station as Tang *et al*. (2009) found. Secondly, with the development of the crack area, the air and water seepage channels are formed inside the surrounding wall rock masses thus the rock bolts and cables would be corroded and invalid. Lastly, the cracks area would induce a leakage of the power house during operation stage.

Up to now, for some fracture phenomena, such as splitting failure, numerous studies (Liu 2009, Yu *et al*. 2015, Wang *et al*. 2014) on crack propagation and stability of rock masses have been conducted for years, as well as numerical methods, which have contributed to the progress of rock mechanics. But there are still many shortcomings and limitations of calculation methods based on the traditional techniques and analytical models. And the mechanical properties of the splitting failure zone in underground surrounding rock masses could not be well-built by traditional constitutive models.

The analysis of this paper is based on field monitoring in Dagangshan Hydropower Station, and a fracture criterion of developed by Shandong University is introduced and applied. Then, a model based on an energy dissipation theory and referencing the mechanical properties of the splitting area of rock masses is established, via calculating the location, depth and the development with the excavation process of the fracturing region. The results show that, this new model is consistent with the situation of the scene, and can be used to be a guide for similar projects to predict the splitting area.

2. Establishment of energy dissipation model

2.1 Secondary development in Flac3D

Flac3D, as a Fast Lagrangian Analysis of Continua medium, which could simulate mechanical behavior of rock, soil, or other material by explicit or implicit finite difference (Chatterjee *et al*. 2015). Flac3D provides a convenient platform for development. Users could customize the new constitutive model and compile *dll* files based on VC++, and then load into Flac3D when

necessary.

2.2 Deformation modulus of rock mass in loading and unloading conditions

Generally speaking, the most obvious feature of brittle rock is that with the increasing of loading and reach to peak strength, afterwards, its stress value will be reduced to a very low level. Specifically, the stress-strain relationship curves have a very steep stress drop. Then the geo-material will have only very low residual strength.

When some elastic brittle mediums such as the rock masses are under compression, many micro cracks in which will be generated after the stress reaches to a level, even the medium is in approximate elastic stage. These micro cracks, will dissipate a lot of energy, which cannot be recovered, including sound, heat and fracture surface energy etc. (Liu and Xiao 2010). After that stage, even it is unloading, the stress-strain relationship of these mediums cannot return to the original status. That is the residual deformation will be happening. Their loading-unloading curves will not overlap, but produce a hysteresis loop, as shown in Fig. 1. The area of the hysteresis loop responses the value of dissipating energy. To make the problem simple, Zhu *et al*. (2011a) assumed that the line of up-going and down-going of the loading-unloading was a straight one, which made convenient calculations.

If energy dissipation in the constitute relation is considered, two cases below should be treated, when the elasto-brittle model is in the process of unloading. For one, it releases by elastic behavior when the element is during the elastic stage. For another, it comes to brittle failure and the rock

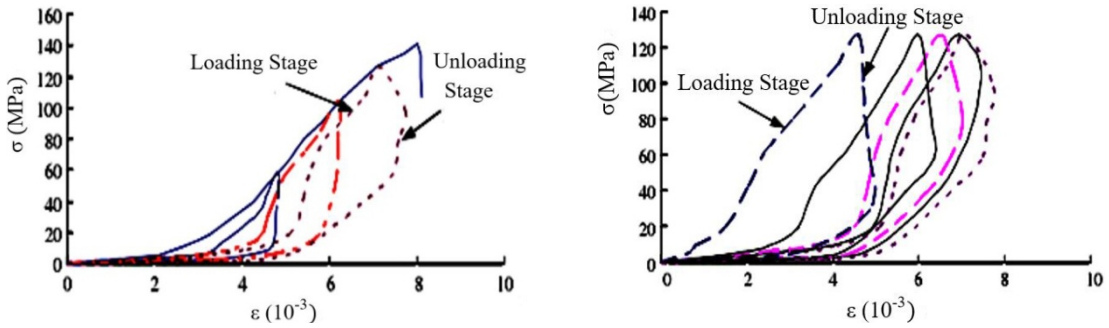

(a) Approximate elastic stage (b) Crack non-steady expansion stage

Fig. 1 Circular loading and unloading curve of rock specimen

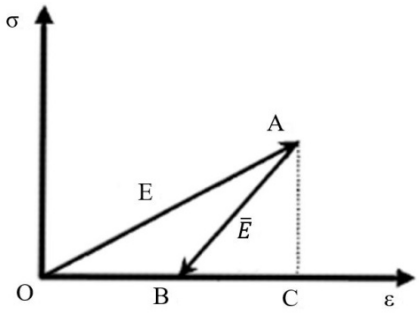

Fig. 2 Stress-strain curve of elasto-brittle model considering energy dissipation

strength decreases after peak stress when the element exceeds the maximum strength. According to the results of the brittle rock mass indoor and field tests by Zhu *et al*. (2014), the loading and unloading process of the elasto-brittle model can be simplified as shown in Fig. 2.

At the loading stage, the elastic modulus is E, and the elastic modulus of the unloading stage becomes to $\overline{E}$. When the specimen is under loading, the strain comes to point A, the specimen absorbs total energy being of S_{AOC}; then at unloading, the strain recovery to point B only, but not the point O, the recoverable energy is S_{ABC}; in this stage, the dissipated energy is S_{AOB}, then

$$\overline{E} = \frac{S_{AOC}}{S_{ABC}} E = \left(1 + \frac{S_{AOB}}{S_{AOC} - S_{AOB}}\right) E \tag{1}$$

Let $1 + \dfrac{S_{AOB}}{S_{AOC} - S_{AOB}} = t$, then $\overline{E} = tE$.

Therefore, when considering the energy dissipation, there is

$$\text{Elastic modulus is} = \begin{cases} \text{loading stage,} & E \\ \text{unloading stage,} & \overline{E} \end{cases} \tag{2}$$

The above theory shows that, the key point for an energy dissipation elasto-brittle model is as following: the model will be adopted different elastic modulus in different stages. The model should use the equivalent elastic modulus $\overline{E}$ when it is at unloading.

The constitutive equations of this model during loading stage is the same with it in Flac3D, but at the unloading stage it is as Eq. (3)

$$\begin{cases} \Delta\sigma_{11} = \overline{\alpha}_1 \Delta\varepsilon_{11} + \overline{\alpha}_2 (\Delta\varepsilon_{22} + \Delta\varepsilon_{33}) \\ \Delta\sigma_{22} = \overline{\alpha}_1 \Delta\varepsilon_{22} + \overline{\alpha}_2 (\Delta\varepsilon_{11} + \Delta\varepsilon_{33}) \\ \Delta\sigma_{33} = \overline{\alpha}_1 \Delta\varepsilon_{33} + \overline{\alpha}_2 (\Delta\varepsilon_{11} + \Delta\varepsilon_{22}) \\ \Delta\sigma_{12} = 2\overline{G}\Delta\varepsilon_{12} \\ \Delta\sigma_{13} = 2\overline{G}\Delta\varepsilon_{13} \\ \Delta\sigma_{23} = 2\overline{G}\Delta\varepsilon_{23} \end{cases} \tag{3}$$

Where: $\overline{\alpha}_1 = \overline{K} + \dfrac{4}{3}\overline{G}$; $\overline{\alpha}_1 = \overline{K} - \dfrac{2}{3}\overline{G}$; $\overline{K}$ is the bulk modulus of unloading stage; $\overline{G}$ is the shear modulus at unloading stage. $\overline{K}, \overline{G}$ could be found from the variable elastic modulus which considering energy dissipation (Zheng *et al*. 2012).

2.3 Criteria for loading and unloading

In this paper, the first and second invariants of the stress tensor are used as the criteria to judge the model is under loading or unloading condition (Zhu *et al*. 2011b, Zheng 2010). Therefore, in this paper, when both the first invariant of the stress tensor (I_1) and second invariant of the stress tensor (J_2) are increasing, the model state is loading. On the other hand, neither I_1 nor J_2 is increasing, we assume that the model is under releasing. Then the loading criterion is as Eq. (4)

$$\left.\begin{aligned} I_1 &= \frac{1}{3}(\sigma_1+\sigma_2+\sigma_3) \\ J_2 &= \frac{1}{\sqrt{2}}\left[(\sigma_1-\sigma_2)^2+(\sigma_2-\sigma_3)^2+(\sigma_3-\sigma_1)^2\right]^{\frac{1}{2}} \end{aligned}\right\} \tag{4}$$

In other cases, when the I_1 and J_2 are no increased or decreased simultaneously, the criteria of model loading-unloading will be determined by the change in status of J_2 as it reflects the deviatoric stress which is playing an important role in rock fracture. Since this criterion could reflect the influence of all three principal stresses on rock stress condition better and could be used as the descriptions of the loading history of rock mass.

According to the above theory, the original model is improved in Flac3D. That is, in the process of solving stress of the element, firstly, judging the stress state of the element by the loading-unloading criterion: if the element is at loading stage, the deformation modulus of the element keep the original modulus E constant, but if the stress state is at unloading condition, the deformation modulus becomes equivalent deformation modulus $\overline{E}$. Secondly, the equivalent deformation modulus $\overline{E}$ of the element based on the effect of energy dissipation and the stress-strain state of the element can be obtained. After that, completing the optimization of user defined constitutive equation based on the development function of Flac3D by VC++. At last, calculating in Flac3D with new function can be conducted.

3. Field monitoring

Dagangshan hydroelectric station, which is the fourteenth of 22 planned cascade hydropower stations of the Dadu River, and is located in the middle reaches of the Dadu River in Shimian, Ya'an, Sichuan Province. The hydropower station is about 40 km from the Shimian City and about 72 km away from Luding City. Its controlled area is 62727 km^2 and occupies 81% of catchment area of Dadu River (Wang *et al*. 2012).

This hydroelectric station has 4 generator units, the capacity of each is 550 MW, with a total capacity of 2,600 MW to ensure the output 636 MW. For many years average generating capacity is 114.5 billion KW·h. The water diversion and power generation system of the hydroelectric station, which includes the main power house, transformer house and tailrace surge chamber, arranged on the left bank of the river. Three large chambers are arranged in parallel, whose axis direction is NE55°, vertical buried depths are 390-520 m and horizontal buried depths are 310-530 m. The total length of the main power house is 226.58 m, the length of the crane girder is 30.80 m, the maximum excavation height of the main engine is 73.78 m, and the elevation of the tail pipe is 920.02 m. The transformer chamber is 144.0 m long, 18.8 m wide, 25.6 m high, and the bottom elevation of the cavern is 962.1 m. The length, width and height of the tailrace surge chamber is 132.0 m, 24.0 m and 75.08 m, respectively, and the bottom elevation of the tailrace surge chamber is 920.02 m (Jia *et al*. 2008).

The type of the surrounding rock of underground powerhouse is mainly grained biotite adamellite (γ24-1), and the surrounding rock partial interspersed with diabase. The rock messes of the plant area is massive and similar-massive structure. There are some weak structural planes such as faults f57, f58, f59, f60 and etc. through the plant caverns.

Generally, there are ②, ③, ④, and ⑤ groups of fracture developed in the rock masses of the plant area of the hydropower station, the length of which are 3-5 m mainly, and some are

longer than 5-10 m individually, and there are some alterations on the surface of the fracture in groups ②, ③, and ④. The steep angle fractures which direction is nearly SN are most developed. The angle between axis of underground powerhouse, which was firstly proposed for NE55°, and σ_1 is small. According to the classification of surrounding rock of Chinese water conservancy trade, the classification of surrounding rock of main power house, transformer chamber and tailrace surge chamber is between Type II and Type III. Overall, the surrounding rocks of the plant area are stable. The results of field monitoring and the reverse calculation show that the geostress field at the underground powerhouse zone is a superposed stress field which is comprised of tectonic stress and gravity stress. The distribution of geostress is affected comprehensively by tectonic stress, geological structure and topography (Zhang *et al*. 2011). This area belongs to the high geostress area (Zhang *et al*. 2009) and the maximum principal stress is up to 26.9 MPa (Li 2009).

In order to obtain the complete information of the deformation and splitting zone of the downstream surrounding rock masses of the main powerhouse during excavation, the authors have pre-set 4 horizontal holes, the depths of which are all 46.5 m or so in the rock masses between the main powerhouse and transformer chamber, so that to make observations of the surrounding rock splitting via the panoramic digital borehole TV convenience. The layout of each hole is shown in Table 1, Figs. 3 and 4.

In order to obverse the rock mass by micro-meter and deformation resistivity instrument, each 2 of these 4 monitoring holes is regarded as a group, including a micro-meter monitoring hole and a deformation resistivity instrument monitoring hole. A3 and A4 are in a group, which are located

Table 1 The position of the monitoring holes

No.	Elevation	Pile No.	Aperture (mm)	Length (m)
A1	963.2	Plant(Horz)0+068.50	110	46.5
A2	963.2	Plant(Horz)0+072.50	110	46.5
A3	963.2	Plant(Horz)0+102.50	110	46.5
A4	963.2	Plant(Horz)0+098.00	110	46.5

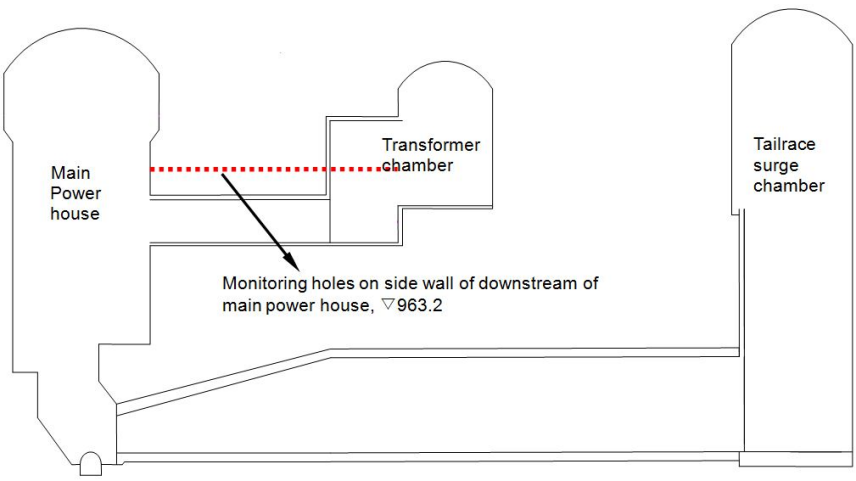

Fig. 3 The elevation and layout of the monitoring holes

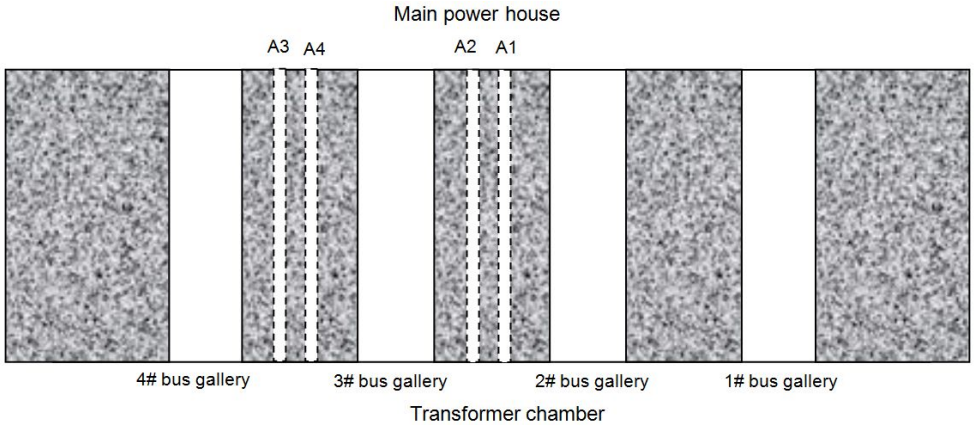

Fig. 4 Layout of the monitoring holes

in the rock masses between 3# and 4# bus gallery, and the two holes is 4.5 m apart. Since the transformer chamber has been already completed and the less interference suffered during the excavation in power house, so that the drilling direction is from the upstream side wall of transformer chamber to the main power house.

The micro-meter was used as the instrument in deformation measurement of surrounding rock, which was imported from a Swiss corporation and had high accuracy (Zhu *et al*. 2011b).

Rock masses deformation will cause the change of its electrical resistivity which can reflect the deformation of the rock masses along the arrangement direction of the electrode system. In this physical premise, the deformation resistivity method is measuring the change of resistivity of rock mass with time based on the characteristics of surrounding rock masses deformation after excavations of the underground cavern to find out the law of rock mass deformation and fracture development.

WDA-1 super digital electric device, the length of the probe is 150 cm, is used in the field resistivity test. The probe has two electrodes, M and A. Three electrodes should be strung around the PVC pipe equally spaced due to them may rotate in drilling, so that it will be ensured that the probes could be in contact with the hole wall in the process. B and N are arranged at infinity, and the generated voltage is measured by M and N electrodes when electrode A and B are producing current.

The digital panoramic borehole camera system is using a kind of domestic production. The monitoring hole in this project is horizontal. The panorama camera probe, which was used as the video recording device was pushed into the monitoring hole by some spindles.

From the field monitoring, three monitoring methods are able to reflect the splitting of the surrounding rock caused by excavation disturbance. As the result of the field monitoring by borehole TV, micro-meter and deformation resistivity instrument shown, the disturbance of the surrounding rock caused by excavation is great. In detail, the depth of the splitting area in surrounding rock masses of downstream of the main power house is greater due to its larger size and the depth of the splitting area in surrounding rock masses of upstream of transformer chamber is relatively small. For 4# generator unit, the depth of the splitting area in surrounding rock masses of downstream of the main power house is significantly larger than that of upstream of transformer chamber.

Due to the differences in measurement accuracy and in anti-interference abilities of these three

Table 2 The depth of the splitting area of the 4# generator unit

Unit section	4# generator unit	
Location	Downstream of the main power house	Upstream of the transformer chamber
Depth of splitting area	13-15 m	5-6 m

monitoring instruments, there are slightly differences between the results obtained by these three instruments, but the overall trend is very consistent. Among the three instruments, the micro-meter as its high accuracy and strong anti-interference ability, the monitoring result obtained by which is most reliable. The other two monitoring methods can be added as supplements. According to the monitoring results, combined with the experience of the project, the depth of the splitting area of the 4# generator unit is shown in Table 2.

The deformation of the side wall at the downstream of main power house of the 4# generator unit is 17-18 mm, and the deformation of the side wall at the upstream of transformer chamber is 5 mm. For such a large underground cavern group, this deformation will not cause obvious instability of surrounding rock masses.

4. Establishment of computational model

4.1 Stress state conditions and prediction formula of the splitting surrounding rock

Li (2007) deduced the criterion for the failure of splitting fracture of rock surrounding by slip crack model.

$$\sigma_1 \geq \frac{K_{IC}\sqrt{\pi L}}{L(\sin\theta\cos^2\theta - \mu\sin^2\theta\cos\theta)} + \sigma_3 \frac{\pi + (\sin\theta\cos^2\theta + \mu\cos^3\theta)}{\sin\theta\cos^2\theta - \mu\cos\theta\sin^2\theta} \tag{5}$$

Where μ is the friction coefficient of initial crack; L is the average length of the initial crack (m); θ is the angle between initial crack and horizontal direction (°); K_{IC} is the fracture toughness (MPa·m$^{1/2}$).

The criterion can be used to predict the depth of the splitting and fracture zone of the surrounding rock masses. To make the formula rationality, it is necessary to assume that the angle between most initial cracks and horizontal direction are large enough.

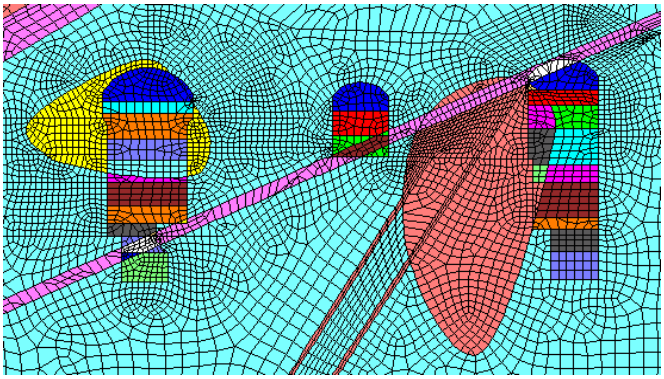

Fig. 5 Quasi-3D model of the 4# generator unit

Table 3 Mechanical parameters of the quasi-3D model of the 4# generator unit

Rock classification	Bulk density (kg/m^3)	Deformation modulus (GPa)	Friction angle (°)	Cohesion (MPa)	Poisson's ratio	Tensile strength (MPa)
II	2650	23.5	52.4	2.0	0.25	8.0
III	2650	9.5	47.7	1.4	0.27	6.0
IV	2650	2.5	38.7	0.7	0.35	4.0
II/III	2650	16.5	50.2	1.7	0.26	7.0

4.2 Calculation model and parameters

In this paper, a quasi-3D model including main power house, transformer chamber and tailrace surge chamber of 4# generator unit is established to calculate and analysis the stability of surrounding rock masses, as shown in Fig. 5. The excavation of the main powerhouse is divided into 8 steps from top to bottom.

According to the results of field monitoring, some experiences and mechanical parameters inversion analysis, the mechanical parameters of the quasi-3D model of the 4# generator unit are adopted and shown in Table 3.

5. Analysis of calculation results

5.1 General analysis of the splitting failure of the surrounding rock

According to the experience and inversion analysis, the main parameters of the Eq. (5) are adopted as follows

$$\mu = 0.2,\quad \theta = 40^{\circ},\quad K_{IC} = 0.84\ \text{MPa}\cdot\text{m}^{1/2},\quad L = 5\ \text{m}$$

Firstly, the parameters are induced into the Eq. (5). By calculating in Flac3D, the principal stress of the surrounding rock masses of the 4# generator unit after each step excavation has been obtained. The splitting area of the 4# generator unit after 6 to 8 step excavation is shown in Figs. 6-8.

Figs. 6-8 show that, the depth of the splitting zone in the surrounding rock masses at downstream of the main power house is larger than it at upstream one. The average depth of the splitting zone in the surrounding rock masses at downstream is approximately 13.6 m, and the

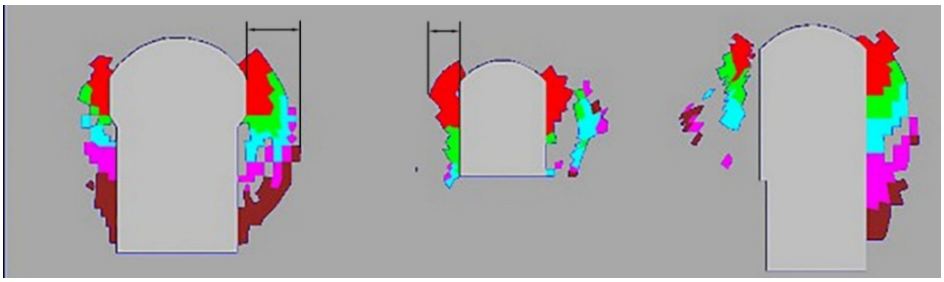

Fig. 6 The splitting area of the 4# generator unit after 6th step excavation

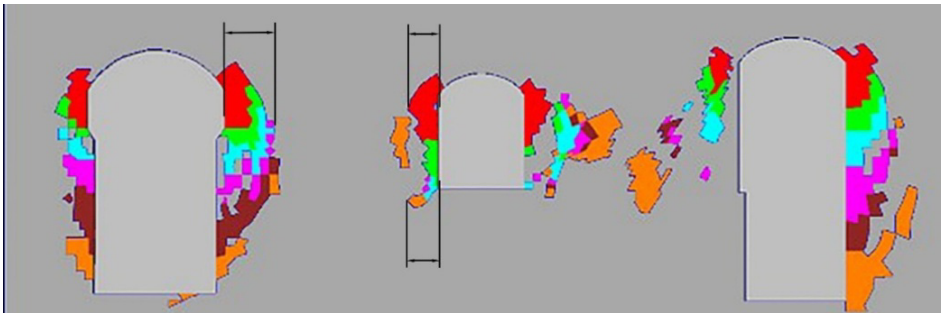

Fig. 7 The splitting area of the 4# generator unit after 7th step excavation

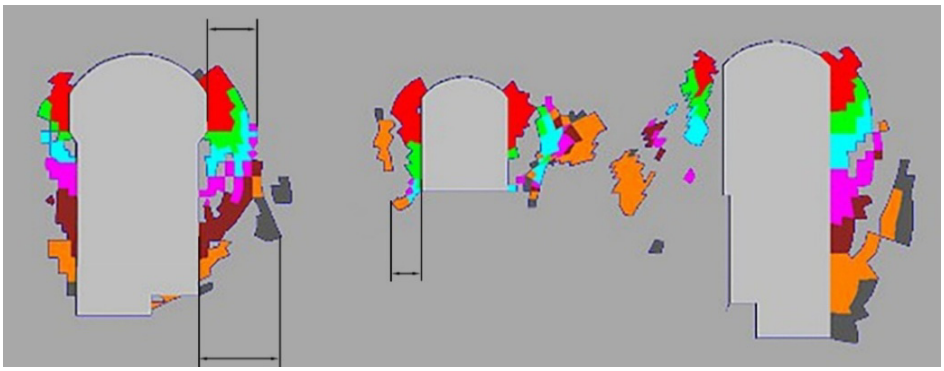

Fig. 8 The splitting area of the 4# generator unit after 8th step excavation

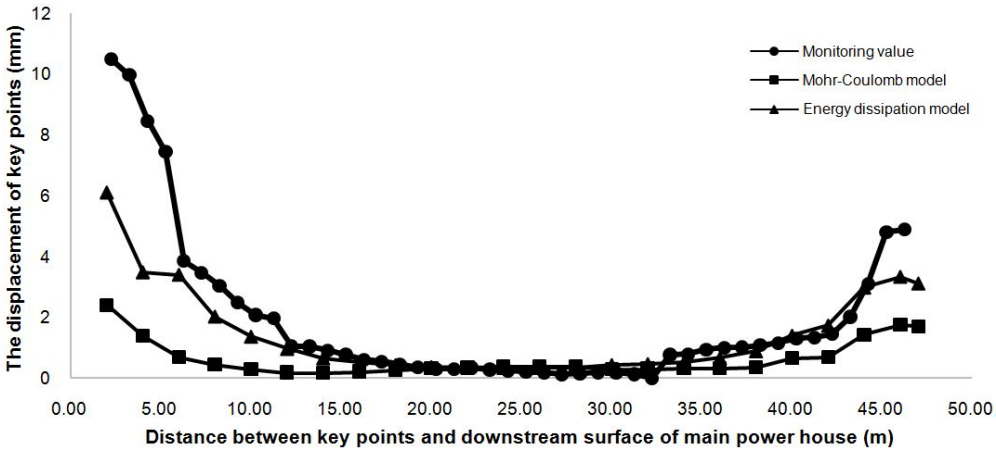

Fig. 9 The displacement of the key points of main power house after 5th step excavation

maximum value of which is approximately 17.4 m. The average depth of the splitting zone in the surrounding rock masses at downstream of the transformer chamber is approximately 6.3 m. The calculation results and the monitoring results are in good agreement.

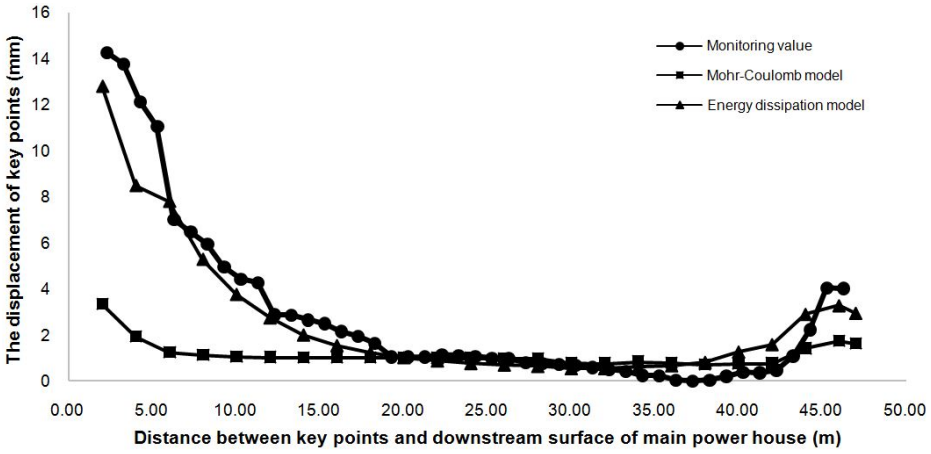

Fig. 10 The displacement of the key points of main power house after 6th step excavation

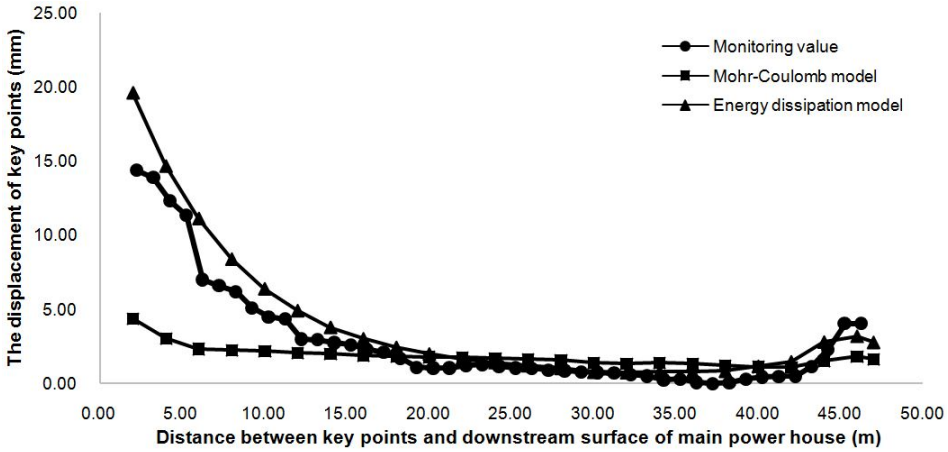

Fig. 11 The displacement of the key points of main power house after 7th step excavation

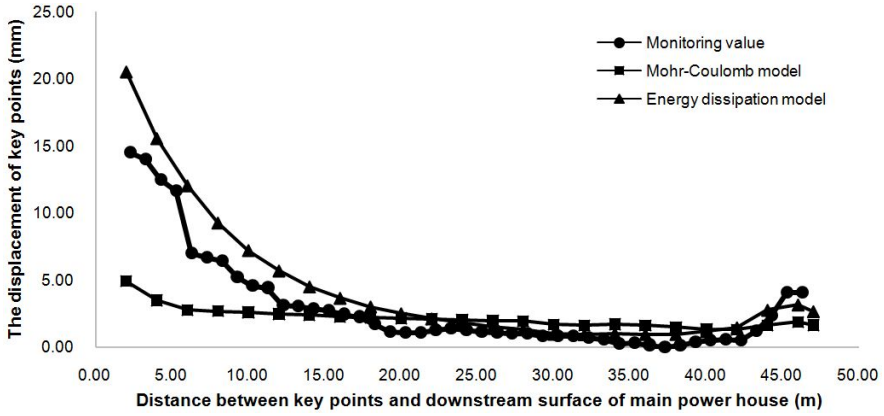

Fig. 12 The displacement of the key points of main power house after 8th step excavation

5.2 Variation analysis of the displacement of surrounding rock displacement

From the model of 4# generator unit, the key points, similar with which in the field monitoring between the main power house and transformer chamber, have been selected, as shown in Fig. 3. And the displacement of each key point has been obtained after calculation. In order to verify the correctness, the results of the calculation are derived and compared with the displacement data of field monitoring, as shown in Figs. 9-12.

From Figs. 9-12, since the cavern sizes of the main power house are larger than those of transformer chamber, more disturbing effects on the surrounding rock are caused by excavations. Therefore, the displacement of the key points near the downstream surface of the main power house is larger than that near the upstream surface of the transformer chamber. After the completion of excavation for the eighth layer of power house, according to the field monitoring, the maximum displacement of surrounding rock, which is the point most close to the surface of the downstream of the main power house, is approximately 14.52 mm. Then, the displacement decreases with the increasing of the distance of measuring point from the main power house downstream surface. When the distance between the main power building and the measuring point is about 15 m, the trend of displacement of surrounding rock is reduced and tends to be stable. When the distance between the measuring point and downstream surface of the main power house is increased up to 41 m, the displacement of surrounding rock gradually increases again and rises to an extreme point when the measure point is 2 m away from the upstream surface of the transformer chamber. After the completion of excavation for the eighth layer of power house, the maximum displacement measured by this position is approximately 4.08 mm.

Via comparison analysis of the calculation results of energy dissipation model and Mohr-Coulomb model, it can be seen that the displacement curves obtained by using the Mohr-Coulomb model in Flac3D are relatively flat, which cannot clearly show the trend that displacement deduced with the distance between key point and downstream surface of main power house increasing, and the maximum of the curve calculated by Mohr-Coulomb model in Flac3D is far less than the actual monitoring value. Meanwhile the calculated displacement of the rock masses between the main power house and transformer chamber is bigger than the field monitoring value. So that, it is not suitable to use the Mohr-Coulomb model to represent the failure characteristics of underground cavern. The comparison analysis also show that, although there still have some acceptable errors, the calculation results of energy dissipation model could not only reflect the trend of the change of the surrounding rock, but the displacement curve is also more similar with the field monitoring result.

From the displacement curve calculated by energy dissipation model, it can be found that there are two deformation mutation points from downstream surface of main power house to upstream surface of the transformer chamber. Respectively, these two deformation mutation points are located in the point where 15 m away from the downstream surface of the main power house and 5 m away from the upstream surface of the transformer chamber, which shows that the depth of fracture area of the main power house is approximately 14 m and the depth of splitting area of the transformer chamber is approximately 5 m. The calculation shows that the depth of splitting area which is obtained by numerical simulation is in good agreement with the field monitoring results.

6. Conclusions

The principle of energy dissipation has been introduced to the constitute relation, and the model

of loading-unloading variable elastic modulus has been developed by secondary development of original constitutive models in Flac3D, which could be used on stability calculation of brittle rock under high geostress. This model could be better than the former Mohr-Coulomb model in numerical simulations on the large deformation caused by splitting failure of joint rock masses.

- Field monitoring of large underground cavern group in the Dagangshan hydropower station has been carried out. The phenomenon of splitting failure caused by excavation disturbance was monitored in 4# generator unit via borehole TV, micro-meter and deformation resistivity instrument, and the field monitoring data were obtained. The monitoring result shows that, the depth of the splitting area in surrounding rock masses of downstream of the main power house is larger than that of upstream of transformer chamber. The depths of the splitting area in surrounding rock masses of downstream of main power house and upstream of transformer chamber are approximately 13-15 m and approximately 5-6 m, respectively. The deformation of the side wall of the downstream of the main power house is approximately 17-18 mm or so and that of the upstream of the transformer chamber is approximately 5 mm.
- A quasi-3D energy dissipation model including main power house, transformer chamber and tailrace surge chamber of 4# generator unit is established to calculate and analyze the stability of surrounding rock masses. The calculation result shows that the average depth of splitting zone in the rock masses of downstream the main power house and upstream the transformer chamber is approximately 13.6 m and 6.3 m, respectively, which is close to the field monitoring result. The key points which between the main power house and transformer chamber on the model are chosen to extract the displacement and compare with the field monitoring value. After comparison, it is found that the calculated displacement curves are in good agreement with the actual monitoring data. Therefore, it can be concluded that this model can simulate the fracture of brittle rock under high geostress. The calculation results show also that the deformation calculated by the previous model are much smaller than the measured value.
- Analysis of the displacement curve can be seen that, when the key point is located at approximately 14 m away from downstream surface of the main power house and approximately 5 m away from upstream surface of the transformer chamber, there appears the displacement mutation point respectively, which means the depth of the splitting zone of the downstream of the main power house is approximately 14 m and the depth of the splitting zone of the transformer chamber is approximately 5 m. The calculation results are in good agreement with the field test results.

Acknowledgments

The work is supported by National Science and Technology Support Program of China (Grant No. 2015BAB07B05), National Natural Science Foundation of China (Grant Nos. 51379112 and 51422904), Fundamental Research Funds of Shandong University (Grant Nos. 2015JX003 and 2016JC007), and Shandong Provincial Natural Science Foundation, China (Grant No. ZR2016EEQ01). Dr. Yong Li is the corresponding author.

References

Chatterjee, K., Choudhury, D., Rao, V.D. and Mukherjee, S.P. (2015), "Dynamic analyses and field observations on piles in kolkata city", *Geomach. Eng., Int. J.*, **8**(3), 415-440.

Hibino, S. and Motojma, M. (1995), "Characteristic behavior of rock mass during excavation of large caverns", *Proceedings of the 8th International Congress on Rock Mechanics*, Tokyo, Japan, September.

Jia, S.P., Chen, W.Z., Tan, X.J. and Lv, S.P. (2008), "Nelder-Mead algorithm for inversion analysis of in-situ stress field of underground powerhouse area of Dagangshan Hydropower Station", *Rock Soil Mech.*, **29**(9), 2341-2349.

Li, X.J. (2007), "Experimental and theoretical studies of formation mechanism of splitting failure of the deep cavern", Ph.D. Dissertation; Shandong University, Shandong, China.

Li, Y. (2009), "Study on the stability induced by stepped excavations and rheological effect of underground cavern groups in high in-situ stress areas", Ph.D. Dissertation; Shandong University, Shandong, China.

Li, X.J., Zhu, W.S., Li, S.C. and Yang, W.M. (2011), "A new displacement prediction method of brittle jointed rock mass considering excavation unloading splitting effect", *Chin. J. Rock Mech. Eng.*, **30**(7), 1445-1453.

Li, Y., Zhu, W.S., Fu, J.W., Guo, Y.H. and Qi, Y.P. (2014), "A damage rheology model applied to analysis of splitting failure in underground caverns of Jinping I hydropower station", *Int. J. Rock Mech. Min. Sci.*, **71**, 224-234.

Li, Y., Guo, Y.H., Zhu, W.S., Li, S.C. and Zhou, H. (2015a), "A modified initial in-situ stress inversion method based on FLAC3D with an engineering application", *Open Geosci.*, **7**(1), 824-835.

Li, Y., Wang, H.P., Zhu, W.S., Li, S.C. and Liu, J. (2015b), "Structural stability monitoring of a physical model test on an underground cavern group during deep excavations using FBG sensors", *Sensors*, **15**(9), 21696-21709.

Li, Y., Zhou, H., Zhu, W.S., Li, S.C. and Liu, J. (2015c), "Numerical study on crack propagation in brittle jointed rock mass influenced by fracture water pressure", *Materials*, **8**(6), 3364-3376.

Li, Y., Zhou, H., Zhu, W.S., Li, S.C. and Liu, J. (2015d), "Numerical investigations on slope stability using an elasto-brittle model considering fissure water pressure", *Arab. J. Geosci.*, **8**(12), 10277-10288.

Li, Y., Zhou, H., Zhu, W.S., Li, S.C. and Liu, J. (2016a), "Experimental and numerical investigations on the shear behavior of a jointed rock mass", *Geosci. J.*, **20**(3), 371-379.

Li, Y., Zhou, H., Zhang, L., Zhu, W.S., Li, S.C. and Liu, J. (2016b), "Experimental and numerical investigations on mechanical property and reinforcement effect of bolted jointed rock mass", *Constr. Build. Mater.*, **126**, 843-856.

Liu, N. (2009), "Study on mechanical mechanism and energy analysis model of splitting failure in high geostress", Ph.D. Dissertation; Shandong University, Shandong, China.

Liu, H.B. and Xiao, M. (2010), "Stability assessment of surrounding rock of underground cavern complexes based on energy-dissipation model", *Asia-Pacific Pow. Energy Eng. Conference*, *APPEEC*, Chengdu, China, March.

Ma, H.L., Yang, C.H., Li, Y.P., Shi, X.L., Liu, J.F. and Wang, T.T. (2015), "Stability evaluation of the underground gas storage in rock salts based on new partitions of the surrounding rock", *Environ. Earth Sci.*, **73**(11), 6911-6925.

Tang, J.F., Xu, G.Y. and Tang, X.M. (2009), "Cause analysis of longitudinal cracks of rock-anchored beam and its developmental trend in underground powerhouses", *Chin. J. Rock Mech. Eng.*, **28**(5), 1000-1009.

Wang, J., Zhu, W.S., Li, S.C., Yang, W.M. and Yu, D.J. (2012), "Study on model test and REV of jointed rock mass and engineering application", *Energy Educ. Sct. Technol. Part A. Energy Sci. Res.*, **30**(SPEC. ISS.1), 1167-1174.

Wang, J., Li, S.C., Li, L.P., Zhu, W.S., Zhang, Q.Q. and Song, S.G. (2014), "Study on anchorage effect on fractured rock", *Steel Compos. Struct., Int. j.*, **17**(6), 791-801.

Wang, H.P., Li, Y., Li, S.C., Zhang, Q.S. and Liu, J. (2016a), "An elasto-plastic damage constitutive model for jointed rock mass with an application", *Geomech. Eng., Int. J.*, **11**(1), 77-94.

Wang, Z.S., Li, Y., Zhu, W.S., Xue, Y.G. and Yu, S. (2016b), "Splitting failure in side walls of a large-scale

underground cavern group: A numerical modelling and a field study", *Springerplus*, **5**(1), 1528.
Yu, S., Zhu, W.S., Yang, W.M., Zhang, D.F. and Ma, Q.S. (2015), "Rock bridge fracture model and stability analysis of surrounding rock in underground cavern group", *Struct. Eng. Mech.*, **53**(3), 481–495.
Zhang, J.G., Zhang, Q.Y., Yang, W.D. and Zhang, X. (2009), "Regression analysis of initial geostress field in dam zone of Dagangshan hydropower station", *Rock Soil Mech.*, **30**(10), 3071-3078.
Zhang, H.Y., Wei, Q., Sheng, Q., Leng, X.L. and Jing, F. (2011), "Three dimensional back analysis of geostress field in underground powerhouse zone of Dagangshan hydropower station", *Rock Soil Mech.*, **32**(5), 1523-1530.
Zheng, W.H. (2010), "The study on opening displacement of brittle rockmass in high geostress", M.S. Dissertation; Shandong University, Shandong, China.
Zheng, W.H., Zhu, W.S. and Liu, D.J. (2012), "Simulation of opening displacement of brittle rockmass at point of energy dissipation", *Rock Soil Mech.*, **33**(11), 3503-3508.
Zhou, X.P., Zhang, Y.X., Ha, Q.L. and Zhu, K.S. (2008), "Micromechanical modelling of the complete stress-strain relationship for crack weakened rock subjected to compressive loading", *Rock Mech. Rock Eng.*, **41**(5), 747-769.
Zhou, X.P., Xia, E.M., Yang, H.Q. and Qian, Q.H. (2012), "Different crack sizes analyzed for surrounding rock mass around underground caverns in Jinping I hydropower station", *Theor. Appl. Fract. Mech.*, **57**(1), 19-30.
Zhu, W.S., Li, Y., Li, S.C., Wang, S.G. and Zhang, Q.B. (2011a), "Quasi-three-dimensional physical model tests on a cavern complex under high in-situ stresses", *Int. J. Rock Mech. Min. Sci.*, **48**(2), 199-209.
Zhu, W.S., Yang, W.M., Xiang, L., Li, X.J. and Zheng, W.H. (2011b), "Laboratory and field study of splitting failure on side wall of large-scale cavern and feedback analysis", *Chin. J. Rock Mech. Eng.*, **30**(7), 1310-1317.
Zhu, W.S., Yang, W.M., Li, X.J., Xiang, L. and Yu, D.J. (2014), "Study on splitting failure in rock masses by simulation test, site monitoring and energy model", *Tunn. Undergr. Space Technol.*, **41**(1), 152-164.

CC